Vision Research 49 (2009) 127–133

Contents lists available at ScienceDirect

Vision Research

journal homepage: www.elsevier.com/locate/visres

Visual evoked spread spectrum analysis (VESPA) responses to stimuli biased towards magnocellular and parvocellular pathways ☆

Edmund C. Lalor [a,b], John J. Foxe [a,c,d,*]

[a] Trinity College Institute of Neuroscience, Trinity College Dublin, Dublin, Ireland
[b] Department of Electrical and Electronic Engineering, Trinity College Dublin, Dublin, Ireland
[c] The Cognitive Neurophysiology Laboratory, Nathan S. Kline Institute for Psychiatric Research, Program in Cognitive Neuroscience and Schizophrenia, 140 Old Orangeburg Road, Orangeburg, NY 10962, USA
[d] Program in Cognitive Neuroscience, Department of Psychology, City College of the City University of New York, 138th Street & Convent Avenue, New York, NY 10031, USA

ARTICLE INFO

Article history:
Received 11 September 2007
Received in revised form 1 August 2008

Keywords:
VEP
EEG
Stimulus contrast
Impulse response

ABSTRACT

Stimulus contrast fluctuations were controlled while the properties of a novel ERP known as the VESPA (Visual Evoked Spread Spectrum Analysis) were examined using data from 8 healthy human subjects. Substantial differences were seen between the morphologies of VESPAs obtained using low contrast stimuli when compared with those obtained using high contrast and full contrast range stimuli. Topographic distributions for both responses are compared and the findings are considered in terms of the response characteristics of the magnocellular and parvocellular visual pathways and the VESPA method itself.

1. Introduction

Responses of the human brain to visual stimuli reflect the integrated activity of distinct neural substreams. Two of these substreams, known as the magnocellular (**M**) and parvocellular (**P**) pathways are defined not only by anatomical differences, but also by the stimuli to which they preferentially respond. For example, **M** cells have a high luminance contrast gain that saturates at high contrasts (greater than ~32%; Kaplan, 1991; Kaplan & Shapley, 1986), while **P** cells have low contrast gain that typically does not saturate (Kaplan, 1991; Kaplan & Shapley, 1986; Tootell, Hamilton, & Switkes, 1988). Also **M** cells favor spectrally broadband stimuli with low spatial frequency and high temporal frequency, whereas **P** cells demonstrate color-opponency and respond best to high spatial frequency and somewhat lower temporal frequency stimuli (Gouras, 1968; Kaplan & Benardete, 2001). As a result of these differing preferences, both subsystems are thought to be responsible for the processing of separate specific attributes of our visual world. As such, it is of interest to study them independently.

Aside from studies designed to gain a better insight into the processing mechanisms of the **M** and **P** pathways in general, each of these subsystems has also been studied in patients with various eye disorders such as retinitis pigmentosa (Alexander, Barnes, Fishman, Pokorny, & Smith, 2004; Alexander, Rajagopalan, Seiple, Zemon, & Fishman, 2005), glaucoma (McKendrick, Sampson, Walland, & Badcock, 2007) and strabismic amblyopia (Davis et al., 2006). Furthermore, **M** pathway function has been reported to be relatively more impaired in neurocognitive disorders such as schizophrenia (Butler et al., 2005, 2007; Foxe, Murray, & Javitt, 2005; Kim, Zemon, Saperstein, Butler, & Javitt, 2005) and dyslexia (Chase & Stein, 2003). The apparent specificity of cellular substream dysfunction in these disorders adds further importance to the study of the substreams in isolation.

Several visual evoked potential (VEP) studies have sought to achieve this by manipulating stimulus characteristics in order to obtain separate, or at least biased, responses to **M** and **P** pathways in humans (e.g., Rudvin, Valberg, & Kilavik, 2000; Valberg & Rudvin, 1997; Zemon & Gordon, 2006). For example, by restricting the contrast of low spatial frequency visual stimuli to below 10%, one can emphasize the response of the **M** pathway (Zemon & Gordon, 2006). The justification for this is based on the fact that the contrast gain of **M** cells at low contrasts is about 10 times that of **P** cells (Kaplan & Shapley, 1986). Similarly, because of the aforementioned saturation of **M** cells at high contrasts, one can emphasize the response of the **P** pathway by restricting the stimulus contrast to above 32%. The manipulation of this particular stimulus characteristic in order to isolate specific channels has also been

☆ Funded by: The U.S. National Institute of Mental Health Grant RO1 MH65350 to J.J. Foxe. Additional salary support for E.C. Lalor was provided through a Fund for Digital Research Programme grant from the Higher Educational Authority (HEA) of Ireland.

* Corresponding author. Address: The Cognitive Neurophysiology Laboratory, Nathan S. Kline Institute for Psychiatric Research, Program in Cognitive Neuroscience and Schizophrenia, 140 Old Orangeburg Road, Orangeburg, NY 10962, USA. Fax: +1 845 398 6545.
E-mail address: foxe@nki.rfmh.org (J.J. Foxe).

0042-6989/$ - see front matter © 2008 Elsevier Ltd. All rights reserved.
doi:10.1016/j.visres.2008.09.032

used in VEP studies involving patients with schizophrenia (Butler et al., 2007; Kim, Wylie, Pasternak, Butler, & Javitt, 2006) and appears to be a promising line of research.

Researchers have also had some success in assessing **M** and **P** contributions to visual responses obtained using noise-based dynamic modeling techniques. In particular, kernel estimation of the multifocal VEP based on binary M-sequence modulation of carefully titrated visual stimuli has led to a number of conclusions about how activity in these subsystems is reflected in responses on the scalp (Baseler & Sutter, 1997; Hood et al., 2002; Klistorner, Crewther, & Crewther, 1997; Maddess, James, & Bowman, 2005). For example, Baseler and Sutter (1997) not only sought to favor contributions from either **M** or **P** pathways by varying contrast, chromatic, spatial and temporal characteristics of the stimuli but also attempted to decompose responses consisting of the first slice of the second order kernel into two additive components whose behavior was consistent with that of **M** and **P** mechanisms. Klistorner et al. (1997), using only contrast variations, examined both first and second order responses. They concluded that the second order responses demonstrated a simple variation with luminance contrast, suggesting that the first slice is predominantly driven by neural elements that have a latency and contrast function that mimic those of the magnocellular neurons of the primate LGN and that the second slice is dominated by a generator whose properties resemble primate parvocellular function.

An alternative noise-based visual evoked response, the VESPA (Visual Evoked Spread Spectrum Analysis) was recently described (Lalor, Pearlmutter, Reilly, McDarby, & Foxe, 2006a). Unlike the standard VEP, this response is obtained using continuously presented stimuli (e.g., a checkerboard pattern). The luminance or contrast of these stimuli is rapidly modulated (e.g., on every refresh of a computer monitor set to 60 Hz) over many narrowly spaced levels by a stochastic signal. Knowledge of this signal allows estimation from the recorded EEG of the linear impulse response of the visual system using least squares estimation (Marmarelis & Marmarelis, 1978). This impulse response is known as the VESPA.

The VESPA has a distinct topography from that of the transient VEP suggesting activation of different neural subpopulations. The abiding characteristic of the early VESPA maps is a persistently delimited focus over midline occipital scalp without any evidence for the characteristic early bilateral spread over lateral occipital scalp regions that is consistently seen for the standard VEP (e.g. Foxe & Simpson, 2002; Gomez-Gonzalez, Clark, Fan, Luck, & Hillyard, 1994; Murray, Foxe, Higgins, Javitt, & Schroeder, 2001). This pattern suggests that the VESPA may favor midline structures such as striate cortex and neighboring retinotopically mapped extrastriate regions, and perhaps also regions in the dorsal visual stream, activation of which are known to produce midline scalp topographies.

The VESPA also differs from the binary M-sequence based method in a number of ways. In particular the VESPA modulation is not binary, but stimulus contrast is varied almost continuously over a range of contrasts using many narrowly spaced contrast levels. Also, the stochastic signal modulating the contrast of the VESPA stimulus is not subject to the same temporal restrictions as an M-sequence (see Methods), giving the VESPA greater flexibility in terms of stimulus design. The interesting VESPA topographies combined with the flexibility of the method, in terms of the characteristics of both the stimuli and the temporal modulation, suggest its utility as a tool for preferentially activating specific visual substreams in relative isolation.

Thus, as a first step, the primary aim of this paper is to compare VESPA responses to stimuli modulated over contrast ranges biased to one substream over another. Specifically, given that **M** pathway dysfunction has been implicated in several disorders, we aim to obtain a VESPA response to low contrast stimuli that may largely index **M** cell activity. This response is compared to the standard VESPA, which, by comparison with responses to stimuli biased toward **P** cells, we conclude mostly reflects **P** cell activity.

2. Materials and methods

2.1. Subjects

Eight (one female) healthy subjects aged 24–30 years participated in this study. All subjects reported normal or corrected-to-normal vision. The experiment was undertaken in accordance with the Declaration of Helsinki and the Institutional Review Board of the Nathan Kline Institute approved the experimental procedures. All subjects provided written informed consent and were paid for their efforts.

2.2. Stimuli

A checkerboard pattern subtending visual angles of 5.25° vertically and horizontally and with equal numbers of light and dark checks was used throughout this study. The refresh rate of the monitor was set to 60 Hz and on every refresh the contrast of the checkerboard pattern was modulated by a non-binary stochastic signal which had its power distributed uniformly between 0 and 30 Hz (Lalor et al., 2006a).

2.3. Experimental procedure

Subjects were seated in a dark room 60 cm from a 17 in. monitor with a mean luminance of 80.9 cd/m^2. Each subject underwent ten VESPA runs of 120 s each, using a checkerboard where each individual check subtended visual angles of 0.65°. For five of these runs (FULL-RANGE) the stimulus was modulated between 0% and 100% contrast. For the other five runs (LOW-CONTRAST) the stimulus was biased to preferentially stimulate **M** cells by limiting the range over which the contrast was modulated to 0–10%.

Three subjects also undertook a further ten runs of 120 s each where the contrast range of the checkerboard was limited to 32–100% in an effort to bias it toward the **P** system. For five of these runs (HIGH-CONTRAST) the parameters of the checkerboard remained as before and for the other five runs (HIGH-CONTRAST_HSF) a higher spatial frequency checkerboard, with individual checks subtending visual angles of 0.26°, was used. This was in order to further bias the stimuli toward **P** cells.

Subjects were instructed to maintain visual fixation on the center of the screen for the duration of each run. Subjects were instructed to keep the number of eye-blinks and all other motor activity to a minimum. A different modulating waveform was used for each run, although, as mentioned, all waveforms had identical statistics. LOW-CONTRAST and FULL-RANGE runs were interleaved for all subjects with HIGH-CONTRAST and HIGH-CONTRAST_SPF runs intermixed for the relevant subjects. Recovery time between runs was typically in the range 1–3 min.

2.4. EEG acquisition and analysis

EEG data were recorded from 168 electrode positions referenced to location Fz, filtered over the range 0–134 Hz and digitized at a rate of 512 Hz using the BioSemi Active Two system. Subsequently, the EEG was digitally filtered with a high-pass filter with passband above 2 Hz and −60 dB response at 1 Hz and a low-pass filter with 0–35 Hz passband and −50 dB response at 45 Hz.

The VESPA is an estimate of the linear impulse response of the visual system (Lalor et al., 2006a). It is based on the assumption that the EEG response to a stimulus, whose luminance or contrast is rapidly modulated by a stochastic signal, consists of a convolu-

tion of that signal with an unknown impulse response plus noise, i.e.,

$$y(t) = x(t) * w(\tau) + noise \quad (1)$$

Given the known stimulus signal $x(t)$ and the measured EEG $y(t)$, the impulse response, $w(\tau)$, i.e., the VESPA, can be estimated using the method of linear least squares. This can be carried out analytically using the following equation,

$$w = \langle x_t x_t^T \rangle^{-1} \langle x_t y_t \rangle, \quad (2)$$

where x_t is a column vector of input stimulus contrast values in a certain window of time around t, y_t is the EEG value at time t and $\langle\rangle$ denotes mean over t. This involves inversion of the input signal's autocorrelation matrix $\langle x_t x_t^T \rangle$. This represents the key difference between the VESPA method and previous noised based estimation methods. In calculating the VESPA it is not necessary for the input signal's autocorrelation function to be a delta function. That is, the VESPA method is a generalization of the standard transient VEP and M-sequence based noise estimation methods in that the autocorrelation matrix involved in the estimation does not need to be diagonal. It should be noted, that biasing the estimate by adding a regularization matrix with terms along or adjacent to the diagonal can help to reduce overall estimation error by greatly reducing the variance (Lalor et al., 2006a). As in that study, the VESPAs in the current paper were regularized using a regularization parameter, λ, of 4.4×10^{-3}. This essentially means that the VESPA is an estimate of the first order Volterra kernel in comparison to the M-sequence method, which results in the first order Wiener kernel (Marmarelis, 2004). This renders a direct comparison between the two methods difficult, however, one important point to note is that the VESPA method allows for stimuli that modulate in a more general way than M-sequences, allowing greater flexibility and environmental validity in stimulus design. In the present study VESPAs were measured using a sliding window of 500 ms of data starting 100 ms pre-stimulus. VESPAs were calculated for each 120 s run and then averaged across runs for each setup.

3. Results

Fig. 1 shows the VESPA responses to the FULL-RANGE and LOW-CONTRAST stimuli at electrode location Oz for each subject as well as the group average at the same electrode. The morphology of the FULL-RANGE VESPAs is highly consistent across subjects and with that of VESPAs presented in earlier studies using similar stimuli (Lalor, Pearlmutter, Reilly, & Foxe, 2006b; Lalor, Yeap, Reilly, Pearlmutter, & Foxe, 2008; Lalor et al., 2006a). The LOW-CONTRAST VESPAs are also highly consistent across subjects, although they differ in morphology from those to the FULL-RANGE stimuli. The FULL-RANGE VESPA has a negative peak around 75 ms, a positive peak around 100–110 ms and another negative peak around 170 ms. The LOW-CONTRAST VESPA appears to have a small positive peak around 50 ms, a strong negative peak centered on 100 ms and another positive peak around 175 ms. The differing morphologies are clearly seen in the group average waveforms.

Fig. 2 shows the topography of the VESPA to the FULL-RANGE and LOW-CONTRAST stimuli at 20 ms intervals from 30 to 250 ms. As with the single waveforms at Oz, the activity across the scalp is seen to be very different between the two stimulus conditions. Onset of the FULL-RANGE response can be seen with the first negative peak occurring around the midline by 70 ms. This is then followed by a positive peak, again with a midline focus, and lasting from 90 to 130 ms. There is some spreading and division of this positivity around 130 ms accompanied by the onset of another negativity at the midline which spreads and splits from by 170–190 ms. The LOW-CONTRAST response appears to exhibit some earlier activity with a very low amplitude positivity evident at the midline around 50 ms. This weak positivity is supplanted by a strong, clear negativity that emerges at the midline around 70 ms. This negativity lasts until after 110 ms with no evident lateralization. At 150 ms a somewhat widely distributed positivity is evident that becomes more focused by 170 ms and is followed by two negative lateralized peaks of activity that last until at least 250 ms. Because of the difference in mean absolute amplitude of the LOW-CONTRAST and FULL-RANGE VESPAs, the topographies of the two conditions are plotted on different scales.

The signal to noise ratio (SNR) of the group average VESPAs at Oz was found to be higher for the FULL-RANGE stimulus (10.5 dB) than for the LOW-CONTRAST stimulus (7.1 dB). This is not surprising given the much lower power of the LOW-CONTRAST stimulus. The mean SNR across subjects was also higher for the FULL-RANGE (7.6 dB) case than the LOW-CONTRAST (5.6 dB). SNR values were determined by defining the signal as the root mean square of the response values in the interval 0–250 ms and the noise as the root mean square of the values in the interval −265 to 0 ms. In order to examine replicability of responses across subjects for both conditions, we calculated the mean correlation between responses from every subject with those from every other subject at electrode Oz in the interval 0–250 ms. A mean value of $r = 0.52$ was found for the LOW-CONTRAST responses, while for the FULL-RANGE responses the value was $r = 0.56$, illustrating that both methods were similarly consistent.

In order to determine the onset latency of the VESPA response for each method, we calculated the 'Global Field Power' (GFP; Lehmann & Skrandies, 1980) of the group average responses at each time point, using all 160 scalp channels. In order to avoid any contamination in this estimate due to smoothing cause by regularization or to variations in the baseline, the GFP was computed on the responses before regularizing and after baseline correcting by subtracting the mean of the responses in the interval −100 to 0 ms. The onset of each response was then defined as the first time point after 0 ms at which the GFP exceeded twice the mean GFP in the −100 to 0 ms interval.

The LOW-CONTRAST response was found to onset at 72 ms with the FULL-RANGE response onsetting at 68 ms. These results agree reasonably well with the topographic maps of Fig. 2, where, according to the GFP values, the low-amplitude positivity that appears over the midline at around 50 ms for the LOW-CONTRAST response is too weak to be confidently classed as part of the response.

Fig. 3 displays the average VESPAs at electrode Oz for the FULL-RANGE, HIGH-CONTRAST and HIGH-CONTRAST_HSF stimuli across the three subjects who undertook all run types. At electrode Oz, the group average FULL-RANGE VESPA was highly correlated with both the HIGH-CONTRAST ($r = 0.79$, $p < 1 \times 10^{-87}$) and HIGH-CONTRAST_HSF ($r = 0.81$, $p < 1 \times 10^{-91}$) VESPAs. The HIGH-CONTRAST and HIGH-CONTRAST HSF VESPAs were also highly correlated ($r = 0.93$, $p < 1 \times 10^{-174}$). These correlation values were calculated by dividing the cross-covariance of the two responses by the square-root of the product of the autocovariance of each of the two responses.

4. Discussion

In this study, we have obtained VESPA responses to a variety of stimuli biased toward specific neural substreams. By restricting the range over which we modulated the contrast of a stimulus to below 10%, we found a dramatically different VESPA response than that obtained when no restricted range was used, i.e., FULL-RANGE stimulus. We conclude that this response reflects activity of the **M** pathway in relative isolation.

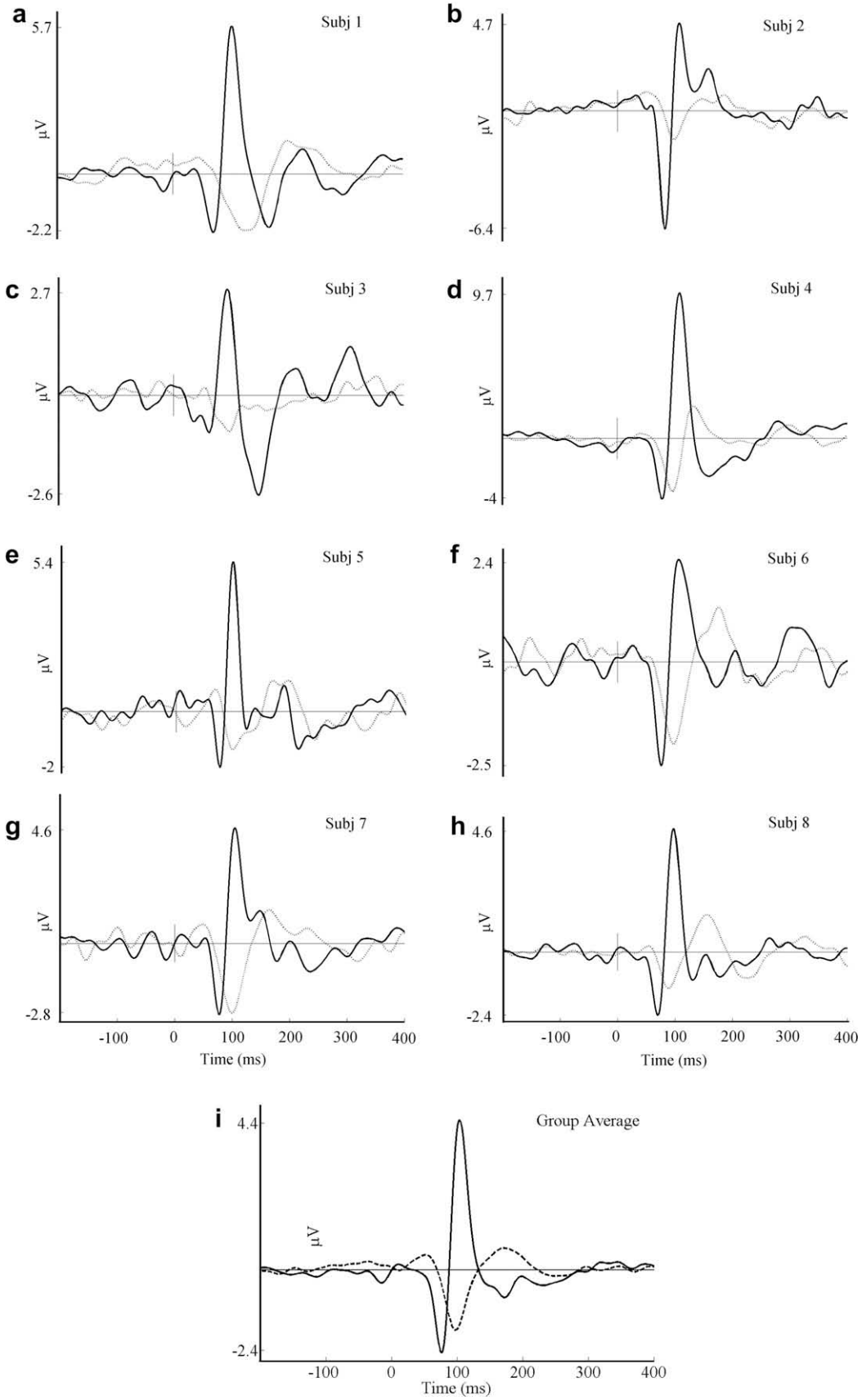

Fig. 1. (a–h) VESPAs elicited using the FULL-RANGE (solid line) and LOW-CONTRAST (dashed line) stimuli for all subjects at electrode location Oz. (i) The group averages.

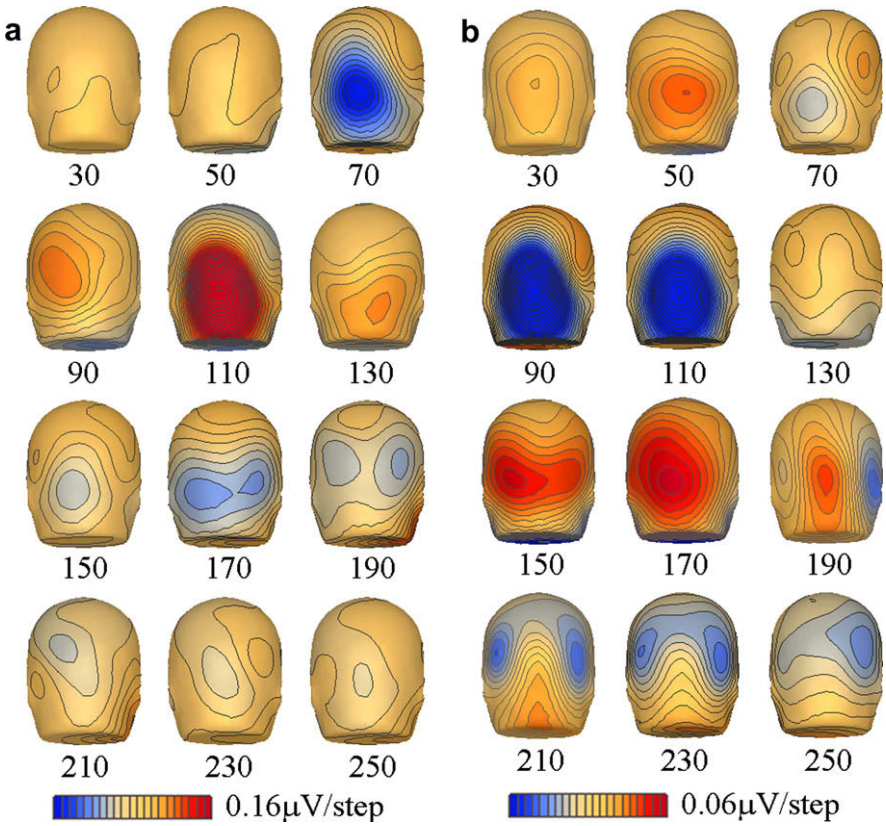

Fig. 2. Scalp topographies for (a) the FULL-RANGE stimulus and (b) the LOW-CONTRAST stimulus. Note the different scales.

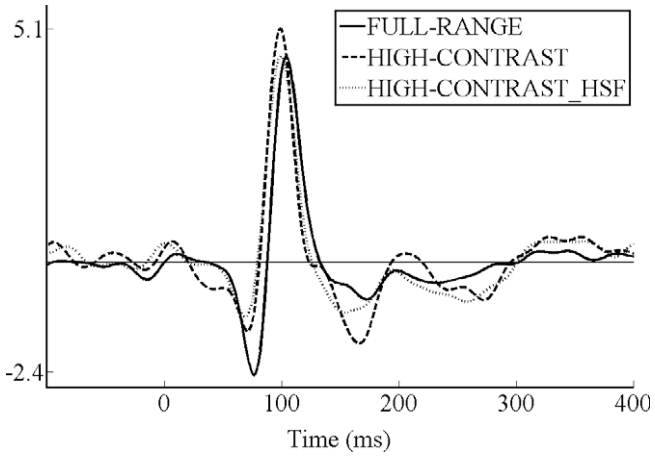

Fig. 3. Group average VESPAs at electrode location Oz elicited using the FULL-RANGE, HIGH-CONTRAST and HIGH-CONTRAST_HSF stimuli.

In contrast, stimuli that were biased towards the **P** pathway elicited VESPAs that were very similar to the FULL-RANGE VESPA. This suggests that the latter is, in fact, largely biased towards **P** cells. This seems sensible when one considers the fact that, because of the mapping of Gaussian noise to contrast level (as detailed in Lalor et al., 2006a), the stimulus used in the FULL-RANGE setup spends over 98% of its time above 10% contrast, where the contrast gain of **M** cells is thought to be lower than that of **P** cells (Kaplan, 1991; Kaplan & Shapley, 1986). It should be noted that all stimulus-modulating signals had the same temporal statistics, and that, by harnessing the flexibility of the VESPA, the cell-specific sensitivity of the analysis could possibly be improved further by shaping those statistics according to the preference of the cell type under investigation, although prior work suggests that the temporal frequency content alone does not significantly affect the VESPA (Lalor et al., 2006b).

With this conclusion in mind we consider the scalp topographies of Fig. 2. This is somewhat complicated by the fact that the anatomically separate **M** and **P** streams are largely recombined by the time they arrive at primary visual cortex (Yabuta, Sawatari, & Callaway, 2001). However, beyond V1, information is still processed in relatively independent dorsal and ventral streams (DeYoe & Van Essen, 1988) with recent evidence suggesting that distinct circuits in V1 relay a fast **M**-dominated signal to area MT in the dorsal stream while a mixed **M** and **P** signal gets relayed to area V2 (Nassi & Callaway, 2007). As a result, one might expect that the responses elicited by the FULL-RANGE and LOW-CONTRAST stimuli used in the present study would have topographies that reflect these differences in processing. For example, one might expect that the response to the LOW-CONTRAST VESPA maps would show a more persistent midline focus moving dorsally over time than the FULL-CONTRAST response. This is not immediately obvious from the topographic maps in that both responses appear to be dominated by strong unimodal foci particularly before 130 ms. Some lateralization can be seen for both methods after 150 ms, however it would be imprudent to make a definitive conclusion about which cortical populations are responsible for each response. One important issue to consider when postulating on which higher cortical areas are activated by the VESPA is that the VESPA analysis assumes that the measured EEG is linearly related to the modulation of the simple luminance or contrast feature of the input stimulus. It is likely that this assumption holds truest for the relatively simple cells of early visual areas, particularly those in striate cortex, and less strongly for complex cells in areas further along the dorsal and ventral streams. This property of the

VESPA could be advantageous in helping to parse out the contributions of each pathway in early visual areas particularly in light of the fact that different contrast response functions have been reported for striate and extra-striate cortex (Hall et al., 2005).

It is believed that the **M** pathway is specialized for detection of motion, whereas the **P** pathway is dedicated to the processing of color, fine detail and, more generally, object recognition (Kaplan, 1991). It is therefore unsurprising that the conduction of information along these pathways differs with the **M** pathway thought to conduct information more quickly than the **P** pathway (Maunsell et al., 1999). In our study, however, we found that the onset time of the response to the LOW-CONTRAST stimulus lagged that of the FULL-RANGE stimulus by about 4 ms. While previous reports have found that the fastest cortical response latencies mediated by **M** channels preceded those of **P** channels by 10 ms (Maunsell et al., 1999), the same report showed that due to the much higher number of parvocellular neurons in the lateral geniculate nucleus (LGN), the **M** channel advantage might be reduced at the cortex by allowing parvocellular signals to generate large detectable responses relatively sooner. Particularly as the present study uses EEG, this notion of a smaller, less easily detected magnocellular driven response may speak to the issue of the weak midline positivity seen around 50 ms for the LOW-CONTRAST stimulus (Fig. 2) that was not classed as part of the response using our GFP-based onset estimation procedure. Furthermore, in the study by Maunsell et al. (1999), slower onset latencies were reported with decreasing luminance, giving another reason as to why the LOW-CONTRAST response might lag the response to the FULL-RANGE stimulus. This relationship between response latency and stimulus contrast has also been seen in EEG studies using the VEP (Spekreijse, van der Twell, & Zuidema, 1973).

There is a substantial difference in the amplitude of the responses to the FULL-RANGE and LOW-CONTRAST stimuli. This is unsurprising given that the ratio of **P** to **M** cells in the fovea has been reported to be as high as 30/1 (Dacey & Petersen, 1992). The reason the discrepancy in VESPA amplitude is not bigger is likely due to the higher contrast gain of **M** cells (Kaplan, 1991; Kaplan & Shapley, 1986).

A couple of cautionary points are worth considering. Firstly, while virtually all studies aimed at biasing responsivity from the **M** and **P** subsystems utilize a contrast manipulation similar to the one described in the present study, many also alter other characteristics of the stimuli such as color and temporal and spatial frequency (e.g., Baseler & Sutter, 1997; Valberg and Rudvin, 1997). Because of the dramatic difference in contrast gain curves between the **M** and **P** pathways (Kaplan, 1991) and the specific manner in which the VESPA stimulus is presented and the VESPA itself calculated, contrast manipulation was the most obvious way to bias responsivity of the two subsystems using the VESPA. Moreover, prior work suggests that color (Lalor, unpublished work) and temporal frequency (Lalor et al., 2006b) manipulations do not lead to the clear dichotomy in responses that we have seen in the present study. However, future investigation, including co-variation of stimulus characteristics may serve to more cleanly bias one subsystem over the other. Secondly, the visual system is highly nonlinear with the **M** pathway being particularly so (Kaplan & Benardete, 2001) and, yet, the VESPA analysis used in the present study is linear. Therefore it is possible that more information on the **M** and **P** subsystems would be revealed by extending the analysis to incorporate nonlinear terms. Such an extension has recently been described (Lalor et al., 2008) and future work will investigate the application of it to isolating the **M** and **P** visual pathways.

In summary, by manipulation of the contrast of a visual stimulus, we have obtained VESPA responses to stimuli biased toward **M** and **P** pathways. These responses, which have high signal to noise ratios, were obtained with a short amount of testing time. With the reported relationship between **M** function and a number of neurological disorders, particularly schizophrenia, this suggests the VESPA as a potentially useful tool in clinical investigation.

Acknowledgment

The authors are grateful to Jennifer Montesi for assistance in gathering the data.

References

Alexander, K. R., Barnes, C. S., Fishman, G. A., Pokorny, J., & Smith, V. C. (2004). Contrast sensitivity deficits in inferred magnocellular and parvocellular pathways in retinitis pigmentosa. *Investigative Ophthalmology and Visual Science, 45*, 4510–4519.

Alexander, K. R., Rajagopalan, A. S., Seiple, W., Zemon, V. M., & Fishman, G. A. (2005). Contrast response properties of magnocellular and parvocellular pathways in retinitis pigmentosa assessed by the visual evoked potential. *Investigative Ophthalmology and Visual Science, 46*, 2967–2973.

Baseler, H. A., & Sutter, E. E. (1997). M and P components of the VEP and their visual field distribution. *Vision Research, 37*, 675–690.

Butler, P. D., Martinez, A., Foxe, J. J., Kim, D., Zemon, V., & Silipo, G. (2007). Subcortical visual dysfunction in schizophrenia drives secondary cortical impairments. *Brain, 130*(Pt 2), 417–430.

Butler, P. D., Zemon, V., Schechter, I., Saperstein, A. M., Hoptman, M. J., & Lim, K. O. (2005). Early-stage visual processing and cortical amplification deficits in schizophrenia. *Archives of General Psychiatry, 62*, 495–504.

Chase, C., & Stein, J. (2003). Visual magnocellular deficits in dyslexia. *Brain, 126*(pt9), E2.

Dacey, D. M., & Petersen, M. R. (1992). Dendritic field size and morphology of midget and parasol ganglion cells of the human retina. *Proceedings of the National Academy of Science of the United States of America, 89*, 9666–9670.

Davis, A. R., Sloper, J. J., Neveu, M. M., Hogg, C. R., Morgan, M. J., & Holder, G. E. (2006). Differential changes of magnocellular and parvocellular visual function in early- and late-onset strabismic amblyopia. *Investigative Ophthalmology and Visual Science, 47*, 4836–4841.

DeYoe, E. A., & Van Essen, D. C. (1988). Concurrent processing streams in monkey visual cortex. *Trends in Neuroscience, 11*, 219–226.

Foxe, J. J., Murray, M. M., & Javitt, D. C. (2005). Filling-in in schizophrenia: A high density electrical mapping and source-analysis investigation of illusory contour processing. *Cerebral Cortex, 15*, 1914–1927.

Foxe, J. J., & Simpson, G. V. (2002). Flow of activation from V1 to frontal cortex in humans. A framework for defining "early" visual processing. *Experimental Brain Research, 142*, 139–150.

Gomez-Gonzalez, C. M., Clark, V. P., Fan, S., Luck, S. J., & Hillyard, S. A. (1994). Sources of attention-sensitive visual event-related potentials. *Brain Topography, 7*, 41–51.

Gouras, P. (1968). Identification of cone mechanisms in monkey ganglion cells. *Journal of Physiology, 199*, 533–547.

Hall, S. D., Holliday, I. E., Hillebrand, A., Furlong, P. L., Singh, K. D., & Barnes, G. R. (2005). Distinct contrast response functions in striate and extra-striate regions of visual cortex revealed with magnetoencephalography (MEG). *Clinical Neurophysiology, 116*, 1716–1722.

Hood, D. C., Yu, A. L., Zhang, X., Albrecht, J., Jägle, H., & Sharpe, L. T. (2002). The multifocal visual evoked potential and cone-isolating stimuli: Implications for L- to M-cone ratios and normalization. *Journal of Vision, 2*, 178–189.

Kaplan, E. (1991). The receptive field structure of retinal ganglion cells in cat and monkey. In A. G. Leventhal (Ed.), *Vision and visual dysfunction* (pp. 10–40). Boston: CRC Press.

Kaplan, E., & Benardete, E. (2001). The dynamics of primate retinal ganglion cells. *Progress in Brain Research, 134*, 17–34.

Kaplan, E., & Shapley, R. M. (1986). The primate retina contains two types of ganglion cells, with high and low contrast sensitivity. *Proceedings of the National Academy of Sciences of the United States of America, 83*, 2755–2757.

Kim, D., Wylie, G., Pasternak, R., Butler, P. D., & Javitt, D. C. (2006). Magnocellular contributions to impaired motion processing in schizophrenia. *Schizophrenia Research, 82*, 1–8.

Kim, D., Zemon, V., Saperstein, A., Butler, P. D., & Javitt, D. C. (2005). Dysfunction of early-stage visual processing in schizophrenia: harmonic analysis. *Schizophrenia Research, 76*, 55–65.

Klistorner, A., Crewther, D. P., & Crewther, S. G. (1997). Separate magnocellular and parvocellular contributions from temporal analysis of the multifocal VEP. *Vision Research, 37*, 2161–2169.

Lalor, E. C., Pearlmutter, B. A., Reilly, R. B., & Foxe, J. J. (2006b). Investigating the temporal frequency characteristics of the human visual system using a system identification approach. In *Proceedings of the 28th Annual International Conference of the IEEE Engineering in Medicine and Biology Society*.

Lalor, E. C., Pearlmutter, B. A., Reilly, R. B., McDarby, G., & Foxe, J. J. (2006a). The VESPA: A method for the rapid estimation of a visual evoked potential. *Neuroimage, 32*, 1549–1561.

Lalor, E. C., Yeap, S., Reilly, R. B., Pearlmutter, B. A., & Foxe, J. J. (2008). Dissecting the cellular contributions to early visual sensory processing deficits in

schizophrenia using the VESPA evoked response. *Schizophrenia Research, 98*, 256–264.
Lehmann, D., & Skrandies, W. (1980). Reference-free identification of components of checkboard evoked multichannel potential fields. *Electroencephalography and Neurophysiology, 48*, 609–621.
Maddess, T., James, A. C., & Bowman, E. A. (2005). Contrast response of temporally sparse dichoptic multifocal visual evoked potentials. *Visual Neuroscience, 22*, 153–162.
Marmarelis, V. Z. (2004). *Nonlinear dynamic modeling of physiological systems*. Hoboken, NJ: Wiley.
Marmarelis, P. Z., & Marmarelis, V. Z. (1978). *Analysis of physiological systems. The white noise approach*. London: Plenum Press.
Maunsell, J. H. R., Ghose, G. M., Assad, J. A., McAdams, C. J., Boudreau, C. E., & Noerager, B. D. (1999). Visual response latencies of magnocellular and parvocellular LGN neurons in macaque monkeys. *Visual Neuroscience, 16*, 1–14.
McKendrick, A. M., Sampson, G. P., Walland, M. J., & Badcock, D. R. (2007). Contrast sensitivity changes due to glaucoma and normal aging: Low-spatial-frequency losses in both magnocellular and parvocellular pathways. *Investigative Ophthalmology and Visual Science, 48*, 2115–2122.
Murray, M. M., Foxe, J. J., Higgins, B. A., Javitt, D. C., & Schroeder, C. E. (2001). Visuo-spatial neural response interactions in early cortical processing during a simple reaction time task: A high-density electrical mapping study. *Neuropsychologia, 39*, 828–844.
Nassi, J. J., & Callaway, E. M. (2007). Specialized circuits from primary visual cortex to V2 and area MT. *Neuron, 55*, 799–808.
Rudvin, I., Valberg, A., & Kilavik, B. E. (2000). Visual evoked potentials and magnocellular and parvocellular segregation. *Visual Neuroscience, 17*, 579–590.
Spekreijse, H., van der Twell, L. H., & Zuidema, T. (1973). Contrast evoked responses in man. *Vision Research, 13*, 1577–1601.
Tootell, R. B., Hamilton, S. L., & Switkes, E. (1988). Functional anatomy of macaque striate cortex IV. Contrast and magno-parvo streams. *Journal of Neuroscience, 8*, 1594–1609.
Valberg, A., & Rudvin, I. (1997). Possible contributions of magnocellular parvocellular-pathway cells to transient VEPs. *Visual Neuroscience, 14*, 1–11.
Yabuta, N. H., Sawatari, A., & Callaway, E. M. (2001). Two functional channels from primary visual cortex to dorsal visual cortical areas. *Science, 292*, 297–300.
Zemon, V., & Gordon, J. (2006). Luminance-contrast mechanisms in humans: Visual evoked potentials and a nonlinear model. *Vision Research, 46*, 4163–4180.